Low cycle fatigue loads

Larsen, Gunner Chr.; Thomsen, K.

Publication date:
1996

Document Version
Publisher's PDF, also known as Version of record

RISØ DK9601647

Risø-R-913(EN)

Low Cycle Fatigue Loads

Gunner C. Larsen and Kenneth Thomsen

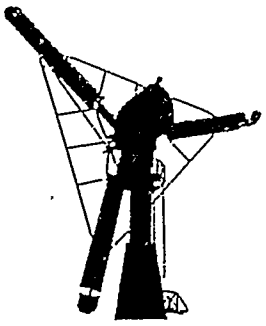

The Test Station
for Wind Turbines

MASTER

Risø National Laboratory, Roskilde, Denmark
August 1996

Low Cycle Fatigue Loads

Risø-R-913(EN)

Gunner C. Larsen and Kenneth Thomsen

Risø National Laboratory, Roskilde, Denmark
August 1996

Abstract The report presents a simple approximative algorithm for taking into account low cycle fatigue loads related to transitions between basic load cases forming the traditional duty cycle description. The algorithm allows inclusion of contributions associated with both transient load cases and production load cases. In the present formulation, the procedure is based on an application of the rainflow counting method as well as the Palmgren–Miner fatigue approach.

The method has been applied to a demonstration example consisting of simulated load events associated with flap– and tilt moments on a wind turbine during a one year period. In the most critical situation, the low–frequency contribution is shown to add approximately 10% to the equivalent moment.

The work has been financially supported by the *Danish Ministry of Energy* under the contract *ENS 1363/94–0002.*

The present report has passed an internal review at The Test Station for Wind Turbines at Risø, performed by:

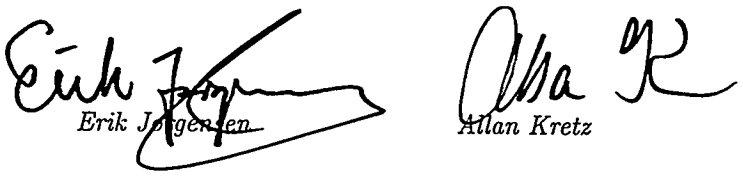

ISBN 87–550–2204–9
ISSN 0106–2840

Grafisk Service · Risø · 1996

Contents

1 Introduction

In this report a simple approximative algorithm for taking into account low cycle fatigue loads is presented.

Traditionally, the fatigue life consumption of a wind turbine is estimated by considering a number of (independent) load cases and performing a rainflow counting analysis on each of those. These results are then subsequently synthesized into a total load spectrum by performing a weighed sum of the number of individual load case ranges. The fatigue life consumption is thus obtained by applying the Palmgren–Miner rule on the total load spectrum.

However, due to the assumption of isolated basic load cases, the above procedure fail to represent the low–frequency contributions related to the transition between those load cases. The procedure to be described in the following aims at taking the fatigue contribution, related to the transitions between the defined load cases, into account in an approximative manner.

2 Definitions

For each of the wind turbine classes I – IV and S in the IEC1400–1 document [1], a *reference year* is introduced as a representative meteorological year with respect to 10–minutes mean wind speed values.

The Weibull distribution is known to describe the distribution of the mean wind speed values with good approximation. The Weibull distribution is defined by only two parametres – a shape parameter and a scale parameter[1].

For the wind turbine classes I – IV, the IEC–standard prescribes the use of a Rayleigh distribution for the mean wind description. However, the Rayleigh distribution is a special case of the Weibull distribution, as the Weibull distribution degenerate to a Rayleigh distribution if the shape parameter 2 and the scale parameter $\frac{2}{\sqrt{\pi}}\bar{U}_a (\approx 1.128\bar{U}_a)$, where $\bar{U}_a$ denotes the annual mean wind speed, are applied.

For the wind turbine class S, it is legitimate to use different shape– and scale parameters. Usually, for annual mean wind speeds larger than roughly 6 m/s (which is of the same order of magnitude as the cut–in wind speed for most wind turbines), the shape parameter takes values in the interval 1.5 to 2.5. As we intend to approximate the effect of low–frequency wind speed variations on the fatigue consumption, a low value of the shape parameter will be conservative[2] as more probalitity is placed in the tails of the distribution in this situation. Consequently a *default shape parameter value* of 1.5 is recommended as a probably conservative

[1] The probability density function describing the Weibull distribution is mathematically expressed as

$$f(\bar{U}) = \frac{k}{A}\left(\frac{\bar{U}}{A}\right)^{k-1} \exp\left(-\left(\frac{\bar{U}}{A}\right)^{k}\right),$$

where $f(\bar{U})$ is the frequency of occurence of mean wind speed $\bar{U}$, k is a shape parameter, and A is a scale parameter.

[2] For $k > 1$, the function has a single maximum up to which it increases monotonically, and after which it decreases monotonically. When k decreases in the interval described by $4.33 > k > 1$, the Weibull function tends to "broaden" thus given rise to increasing variability. This is also seen directly from the analytical expression for the mean square (m.s.) of the function, given by

$$m.s. = A^2\Gamma\left(1+\frac{2}{k}\right),$$

where $\Gamma(\cdot)$ denotes the gamma function.

value for the reference year with respect to low cycle fatigue consumption. As for the scale parameter, the value (assuming $k = 1.5$) resulting in the design annual mean wind speed, characteristic for the particular S–class application, must been selected. The scale parameter is thus in this case obtained from

$$A = \frac{\bar{U}_a}{\Gamma\left(\frac{5}{3}\right)}, \tag{2.1}$$

where $\Gamma(\cdot)$ denotes the gamma function.

3 Synthetic time series

The basic idea is to supplement the total load spectrum, as evaluated based on a number of isolated basic load cases, with a low–frequency contribution obtained from a synthetic load series.

To create a particular synthetic load series, the reference meteorological mean wind speed year, related to the relevant wind turbine class, is utilized. The algorithm has the following steps:

- The 52560 10–minutes mean wind speed values, constituting the reference year, are ordered chronological as illustrated in the figure below.

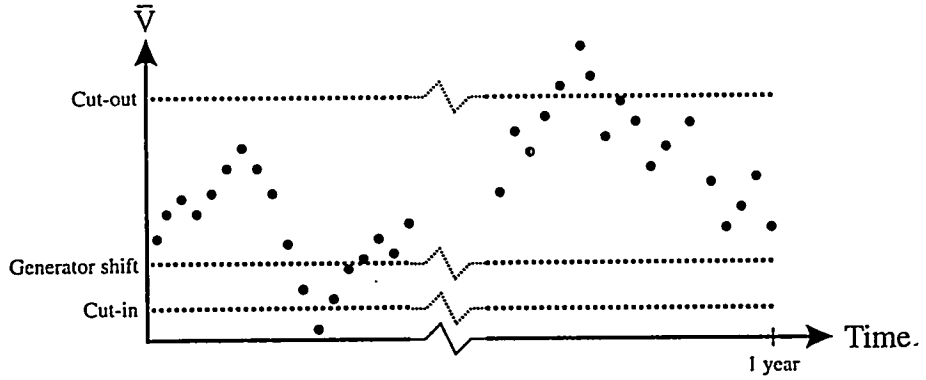

Figure 1. 10–minutes mean wind values related to the reference year.

It is here implicitly *assumed* that one year of 10–minutes mean wind velocities constitute a statistical significant basis for the low cycle load fatigue evaluation.

- The relevant structural response, related to the load cases defined in the IEC1400–1 document, are established by means of aeroelastic simulations and/or by measurements. Note, that some of the (production) load cases may require more that one 10–minutes time series (typically between 3 and 6), primarely due to the demand for sufficient statistical significance of the low–frequency turbulence contribution to the fatigue life consumption (related to an isolated load case).
- For each of the load case time series, the global maximum and minimum values are identified, extracted and saved in the order they appear. Note, that load cases in this respect include normal procuction load cases, start/stop situations, shift between generators, stand still loads at high wind speeds, stand still loads at low wind speeds, etc.. For the production load case no. i (in this case consisting of 6 10–minutes time series), the procedure is illustrated in the figure below.

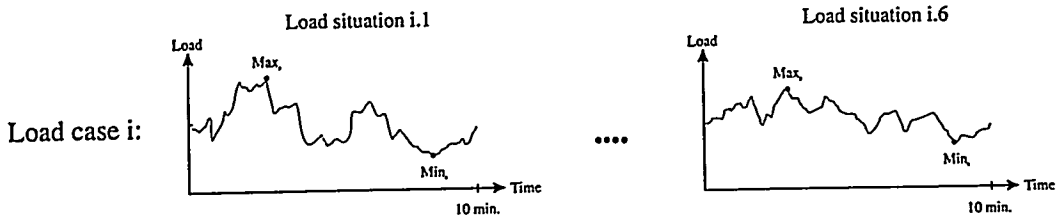

Figure 2. Identification of global extremes of 6 elementary load situations related to production load case no. i.

- The mean wind values contained in the reference year is now examined successively, starting with the first 10–minutes mean value. For each mean velocity value, the relevant load case[3] is identified and it is furthermore examined whether the transition from the previous to the present load case give rise to sublementary transient load cases (start/stop, shift between generators, etc.). Having identified the relevant involved load situations, the corresponding extreme values are transferred to the synthetic structural response time series in the order they appear.
  In case a load case is described by more than one 10–minutes series (as f. ex. the one illustrated in Fig. 2 above), a cyclic procedure is adopted as the first series is used first time the particular load case appear, the second series is used the second time the particular load case appear, etc.. When the last time series related to the particular load case has been utilized, the first time series related to the same load case is applied next time the particular load case appears.
- Considering all the 10–minutes mean wind speed values belonging to the reference year in the above described manner, a synthetic low–frequency structural response time series is constructed. The final result is illustrated in the figure below, where N denotes the total number of load cases considered, in the above described sence, during the reference year.

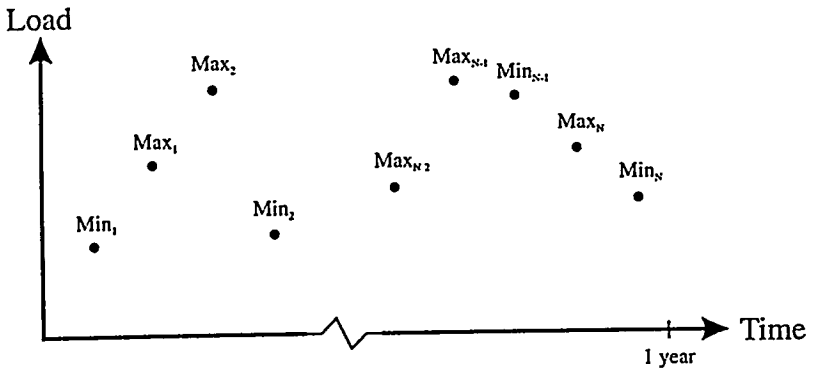

Figure 3. Resulting load time series describing the low–frequency load content.

[3] As for the production load cases, the production wind interval is subdivided into a number bin intervals, typically with a width of 2 m/s. Each load case, belonging to a particular bin, is then described by *one* load case representative for the entire bin interval. This representative load case is often taken as being related to the mean wind speed in the bin interval.

4 Modified total load spectrum

Performing a rainflow analysis on the synthetic load response time series, constructed along the lines described above, results in the desired approximation of the low–frequency contribution to the load spectrum. The result can be added directly to the total load spectrum obtained in the traditionel manner, and a modified total load spectrum emerges which in an approximative manner treat the low–[4] as well as the high frequency load cycles experienced during the lifetime of a wind turbine.

5 Demonstration example

In order to evaluate the influence, primarily on the load spectrum but also on the fatigue evaluation, from taking the low frequency fluctuations into account, an example has been analysed. The reference year of 10–minutes mean wind speed values has (rather arbitrary) been selected as a monitored series from 1995 originating from the Great Belt Experiment, conducted on the island Sprogø in the middle of the Great Belt between the islands Zealand and Funen in Denmark.

The wind data refer to a position 70 m above average sea level. In order to obtain values corresponding to the hub level of the selected wind turbine (Micon M1500–750kW/150kW), the mean wind speed profile is *assumed* to follow the potential law

$$\bar{U}(z) = \bar{U}(z_{ref}) \left(\frac{z}{z_{ref}} \right)^{0.14} , \tag{5.1}$$

where $\bar{U}(z)$ denotes the mean wind speed at hight z above average sea level. The value at hub level is thus expressed as :

$$\bar{U}(40m) = \bar{U}(70m) \left(\frac{40m}{70m} \right)^{0.14} . \tag{5.2}$$

The time series of the mean wind speed corresponding to a position 40 m above average sea level is presented in Fig. 4 below. Note, the distinct seasonal variation with high wind speeds in the winter period, and lower wind speeds in the summer period.

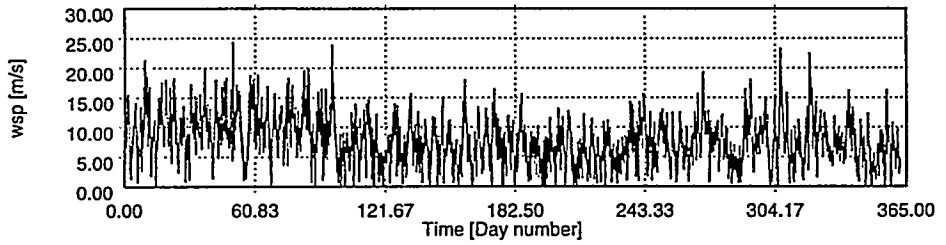

Figure 4. One year of 10–minutes mean wind speed values at level 40 m.

[4] In case a particular material is not sensible to low–frequency fatigue contributions, this must be taken care of in the fatigue evaluation model. Hence, in this situation, the Palmgren–Miner approximation must either be modified or substituted by an other model. A more heuristic approach is to apply a high–pass filter, with appropriate filter characteristics, on the synthetic load response time series before performing the rainflow analysis, and then subsequently apply the traditional Palmgren–Miner approximation on the filtered result. However, the last procedure has the drawback that it is necessary to produce a "wrong" load spectrum in order to obtain a satisfactory description of the fatigue consumption.

A propability distribution, describing the occurence of a particular mean wind speed value, has been estimated based on a binning of the above time series. A Weibull distribution has been fitted to the result by a maximum likeness procedure, and the result is given in Fig. 5 below. The Weibull parameters corresponding to the fit were A = 8.8 m/s and k = 2.31, and as seen a convincing agreement between measured and estimated values is obtained.

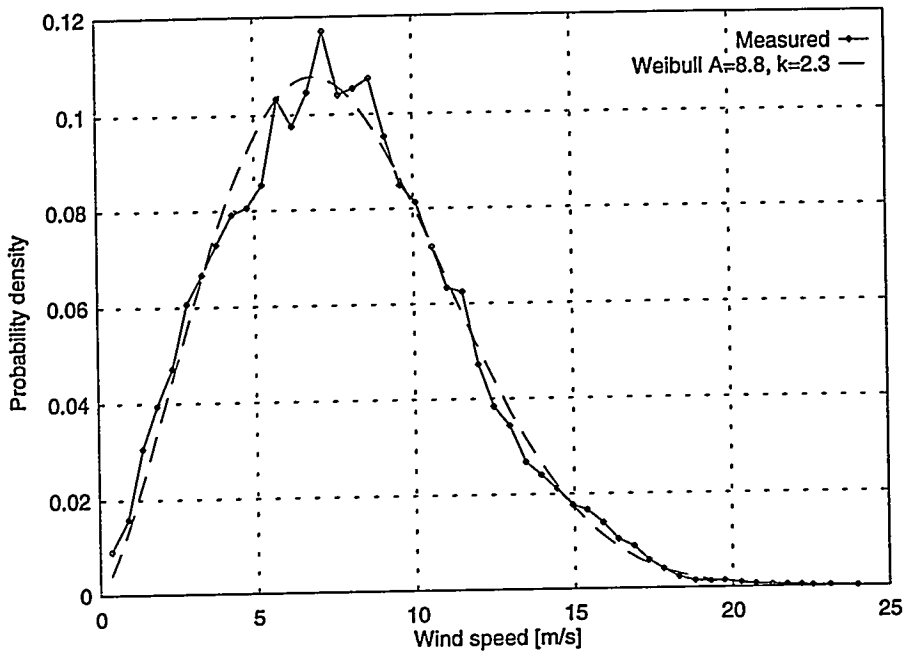

Figure 5. Measured and estimated probability density functions of average mean wind speeds.

The wind turbine selected for the example is, as mentioned above, the Micon M1500–750kW/150kW turbine equipped with LM19.1 blades. For this turbine, the cut–in wind speed is 3 m/s and the cut–out wind speed is 25 m/s. Load cases related to the blade flap moment and to the rotor tilt moment, referring to both production and transient situations (start/stop), have been simulated with an aeroelastic model. The tilt moment relates to the point of intersection between the axis of rotation of the rotor and the centre line of the tower, and the flapwise moment relates to the point at rotor radius 1.5 m. The load cases related to stand–still situations has been neglected in the present study, but could equally well have been included.

For the production load cases, the production wind interval [3 m/s;25 m/s] is subdivided into 11 bin intervals each with a width of 2 m/s. The turbulence intensity is assumed equal to 17%, in accordance with the specifications in the IEC1400–1 document, and zero yaw error was furthermore presumed. Thus, the mean wind interval [3 m/s;5 m/s] is characterized by a simulation with the mean wind speed 4 m/s, the mean wind interval [5 m/s;7 m/s] is characterized by a simulation with the mean wind speed 6 m/s, and so forth.

Three transient load situations have been evaluated corresponding to a start at the cut–in wind speed, a start at the cut–out wind speed, and to a stop at the cut–out wind speed. The load situation corresponding to a stop at the cut–in wind speed introduces very modest loads, and is *assumed* resonably well described by the load case corresponding to the start at the cut–in wind speed.

5.1 Blade flap moment

The main characteristics of the simulated flap moments is summarized in Table 1, where $\bar{U}$ denotes the mean wind speed related to a particular simulation, and T the corresponding length of the simulation.

Load case type	$\bar{U}$ [m/s]	T [s]	Mean [kNm]	Rms [kNm]	Min. [kNm]	Max. [kNm]	Max.-Min. [kNm]
production	4	300	109.6	19.25	36.73	164.8	128.0
production	6	300	167.9	31.03	48.28	253.1	204.8
production	8	300	231.0	39.81	69.43	337.9	268.5
production	10	300	282.3	41.24	94.37	408.8	314.4
production	12	300	313.4	39.20	117.6	449.3	331.7
production	14	300	330.9	38.79	140.3	484.8	344.5
production	16	300	343.5	40.37	162.6	512.5	349.9
production	18	300	355.8	43.12	183.3	545.4	362.1
production	20	300	369.5	46.91	197.4	565.0	367.6
production	22	300	385.4	51.67	192.7	600.9	408.3
production	24	300	403.3	57.30	193.4	636.7	443.3
start; cut–in	3	100	64.34	52.19	10.99	218.9	208.0
start; cut–out	25	100	225.1	92.92	14.17	468.2	454.0
stop; cut–out	25	30	314.8	122.2	40.29	711.5	671.2

Table 1. Main characteristics of the flap moment simulated at $R = 1.5$ m.

As described above, the extreme values, related to the selected load cases, must be transferred to the synthetic structural response time series in the order they appear[5]. However, for the production load cases the same seed–value (in the turbulence simulation) was used for all simulations, resulting in only a scaling of the turbulence for different load cases and thus obviously the same sequencing of the minimum– and the maximum structural loads. In order to compensate for that, a random selection of the sequencing of these extrema was performed. The resulting low–frequency synthetic time series, related to the flap moment at R = 1.5 m, is shown on Fig. 6 below.

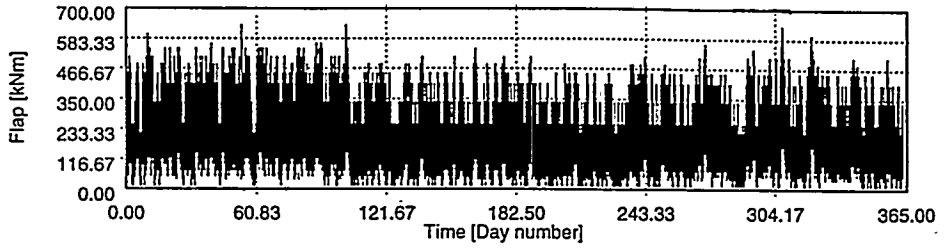

Figure 6. Synthetic time series containing the low–frequency contributions to the flap moment at $R = 1.5$ m.

Based on the above 11 production load cases, a traditional one–year load spec-

[5]For the present purpose (rainflow analysis), a frequency analysis of the synthetic time series is of no relevance, and therefore the load values have been transferred to the synthetic series with equidistant time separations rather than with the true time separations.

trum is is established by considering the load cases as being independent, performing a rainflow counting analysis on each of those, and then subsequently add the results as a weighed sum of number of occurences related to individual load ranges. The weight parameters are the probalitities attached to the particular load cases, determined from the estimated Weibull distribution presented in Fig. 5 (A = 8.8 m/s, k = 2.31), multiplied by the number of 10 minutes sequences contained within a year.

The low–frequency contribution originating from the transitions between the considered load cases, as based on the measured reference year, is taken into account by performing a rainflow counting analysis on the low–frequency synthetic time series presented in Fig. 6 and subsequently add the result directly to the traditional load spectrum described above. The resulting traditional– and total load spectrum are presented in Fig. 7 below.

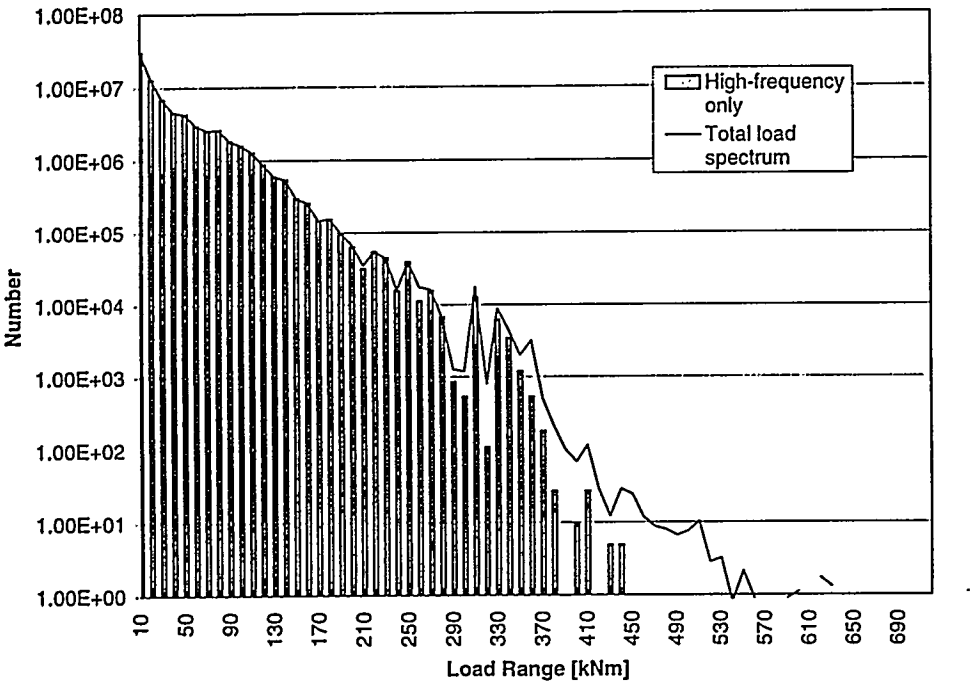

Figure 7. Traditional– and total one year load spectra for the flap moment at R = 1.5 m (not accumulated).

As all the 10–minutes mean wind speed values, constituting the selected reference year, are below the cut–out wind speed (25 m/s) and as the transient situations related to the cut–in wind speed introduce only moderate load ranges, the added low frequency contribution originates mainly from transitions between the basic load cases.

In Fig. 8 the similar results are displayed in terms of accumulated load spectra, where the the number of cycles related to a load range expresses the number of load ranges *larger* than the particular load range.

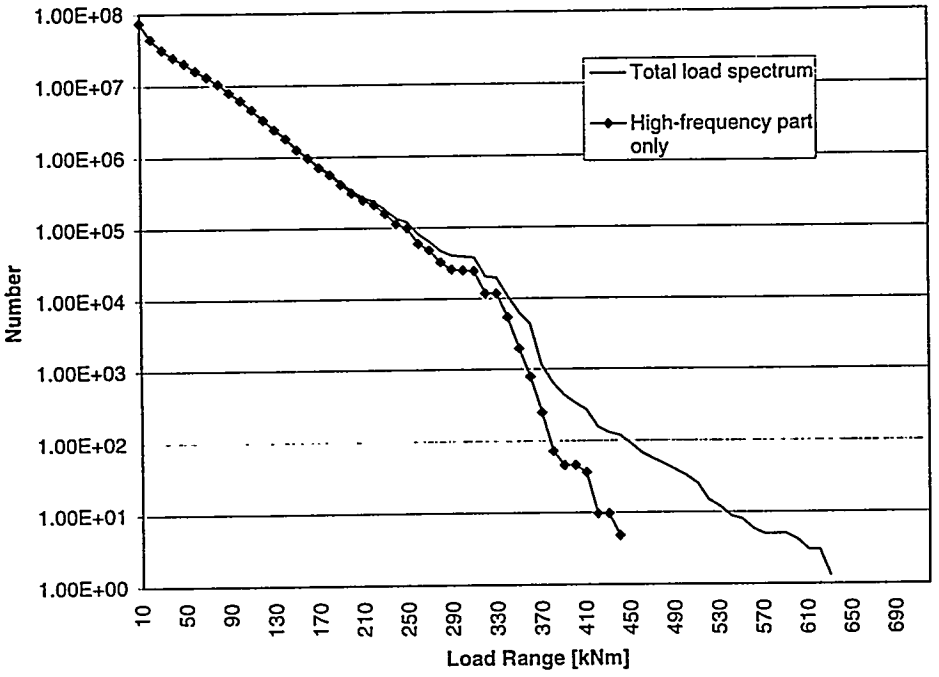

Figure 8. Traditional– and total accumulated one year load spectra for the flap moment at $R = 1.5$ m.

Comparing the traditional– and the total load spectrum, it appears that the parts related to moderate range sizes are very similar, whereas the parts associated with large load ranges differ considerably.

In order to quantify the impact of including the low–frequence contribution in the load spectrum in terms of fatigue life consumption, equivalent load ranges (based on an equivalent number of load ranges equal to 10^6) are established by applying the Palmgren–Miner rule both on the traditional load spectrum and on the total load spectrum. In order to cover a broad range of materials, the Wöhler exponents m = 3, m = 7, and m = 12 were (arbitrary) selected. The results appear from Table 2 below.

m	Traditional load spectrum	Total load spectrum	Ratio
3	277.67 kNm	280.84 kNm	1.01
7	221.01 kNm	230.27 kNm	1.04
12	245.87 kNm	264.72 kNm	1.08

Table 2. Equivalent flap load ranges based on traditional– and total load spectra for various Wöhler exponents.

From Table 2 the damage ratios, corresponding to the listed ratios of equivalent load ranges, are determined to 1.03, 1.33, and 2.43, respectively.

The relative importance of the load ranges in terms of fatigue life time consumption is illustrated on Fig. 9, Fig. 10, and Fig. 11 for different values of the Wöhler exponent. Each of the figures show the relative life time consumption of a particular load range compared to the total fatigue life time consumption related to the specific load spectrum.

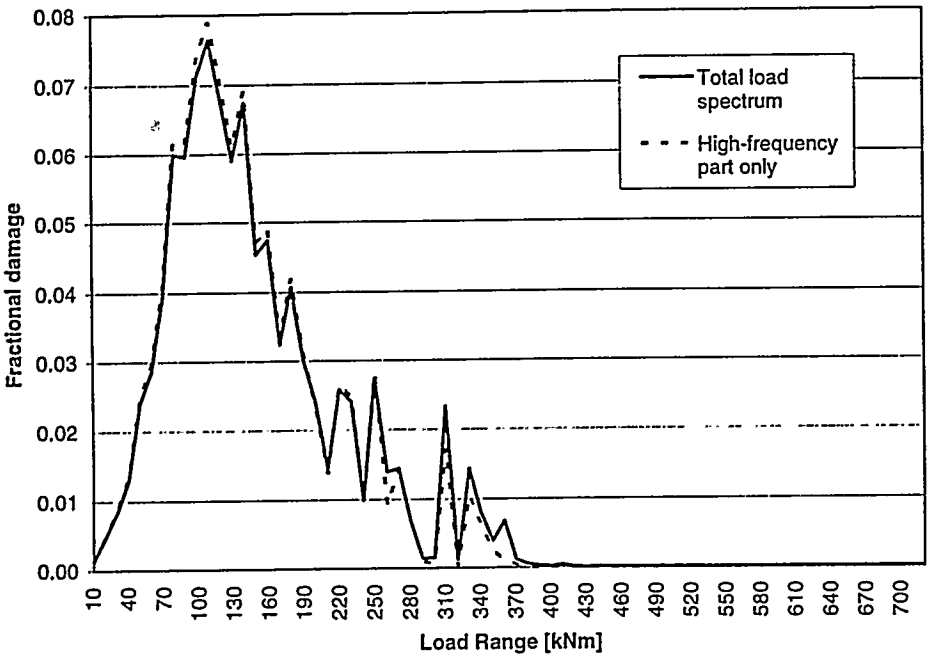

Figure 9. Relative fatigue lifetime consumption for the traditional- and the total load spectrum for $m = 3$.

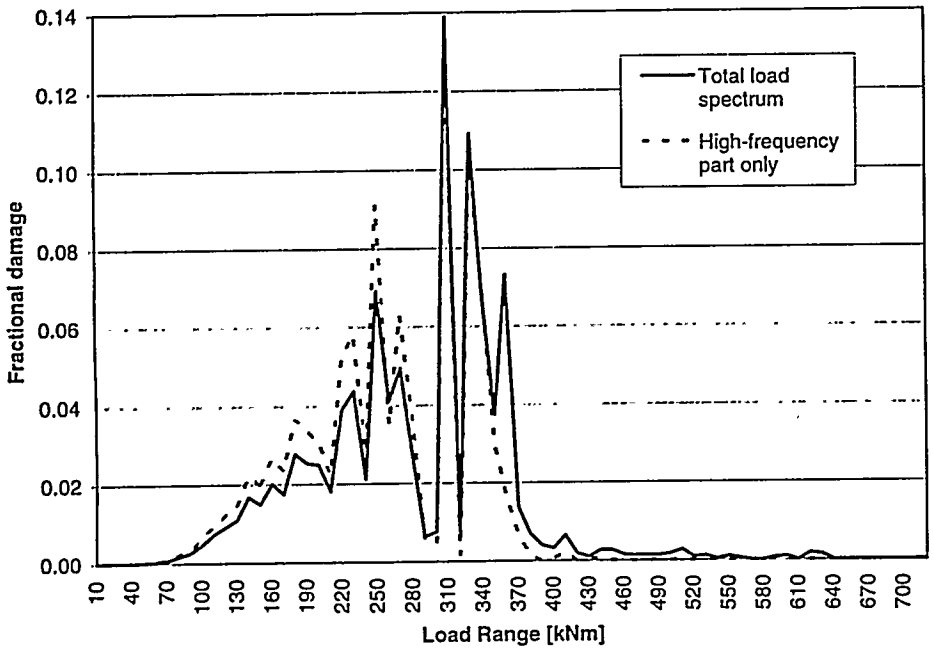

Figure 10. Relative fatigue lifetime consumption for the traditional- and the total load spectrum for $m = 7$.

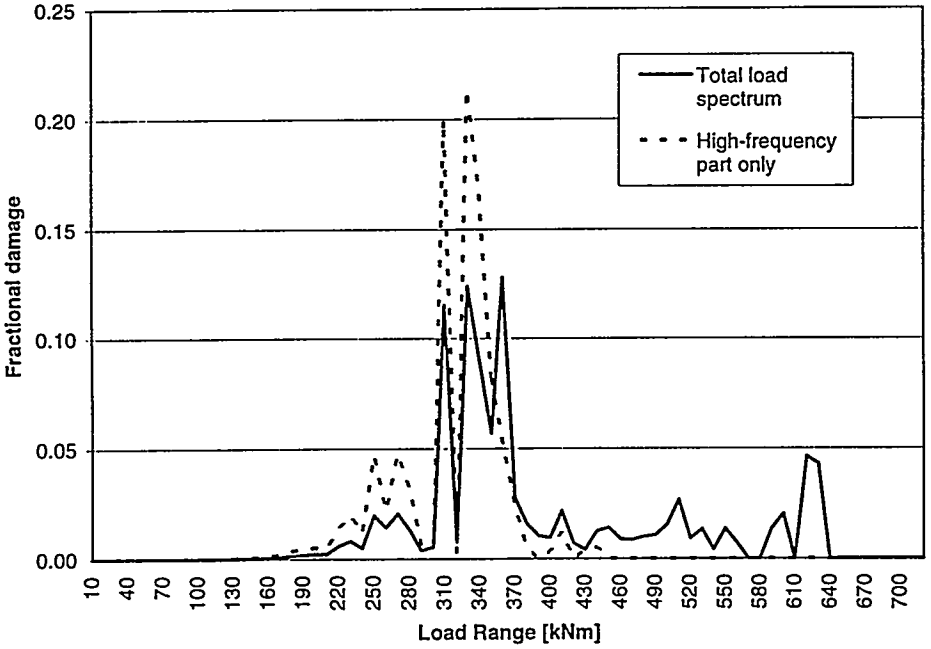

Figure 11. Relative fatigue lifetime consumption for the traditional– and the total load spectrum for $m = 12$.

As mentioned above, the main difference between the traditional– and the total load spectrum is attached to a relative limited number of relative large load ranges. On this background, it is not surprising that the most noticeable difference in curves describing the relative lifetime consumption is obtained for large values of the Wöhler exponent.

5.2 Rotor tilt moment

The main characteristics of the simulated tilt moments is summarized in Table 3. The notation is as previously described.

Load case type	$\bar{U}$ [m/s]	T [s]	Mean [kNm]	Rms [kNm]	Min. [kNm]	Max. [kNm]	Max.-Min. [kNm]
production	4	300	-109.9	24.31	-197.8	-31.58	166.2
production	6	300	-104.5	34.99	-227.2	6.610	233.8
production	8	300	-100.9	43.99	-235.7	44.03	279.7
production	10	300	-102.3	49.43	-259.9	69.12	329.0
production	12	300	-107.5	54.98	-287.7	68.14	355.9
production	14	300	-111.5	60.85	-338.9	100.3	439.2
production	16	300	-113.3	66.94	-366.5	124.4	490.9
production	18	300	-113.2	72.42	-376.5	147.4	523.9
production	20	300	-111.8	77.91	-388.7	164.3	553.0
production	22	300	-109.6	83.89	-424.9	176.4	601.3
production	24	300	-107.0	90.44	-456.8	179.9	636.7
start; cut-in	3	100	-120.0	16.71	-197.3	-43.75	153.6
start; cut-out	25	100	-104.3	67.96	-392.1	125.4	517.4
stop; cut-out	25	30	-102.7	98.37	-398.6	161.3	559.9

Table 3. Main characteristics of the simulated rotor tilt moment.

As with the flap moments, the extreme 10 minutes tilt values have been transferred to the synthetic series with equidistant time separations and with a random selection of the sequencing of these extrema. The resulting low-frequency synthetic time series related to the tilt moment is shown on Fig. 12.

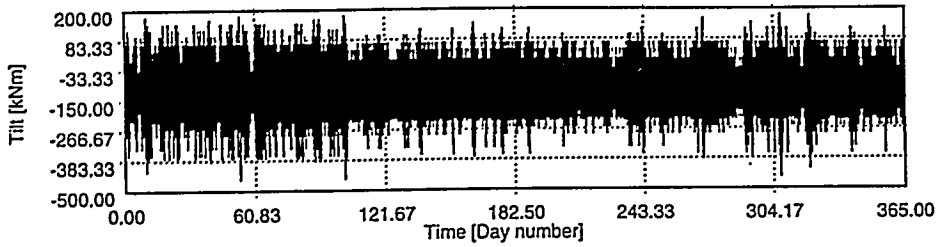

Figure 12. Synthetic time series containing the low-frequency contributions to the tilt moment.

Adopting the same procedure as for the flapwise blade moments, the traditional one-year tilt load spectrum and the low-frequency contibution, originating from the transitions between the considered load cases, for the tilt moment are determined. The result is shown in Fig. 13.

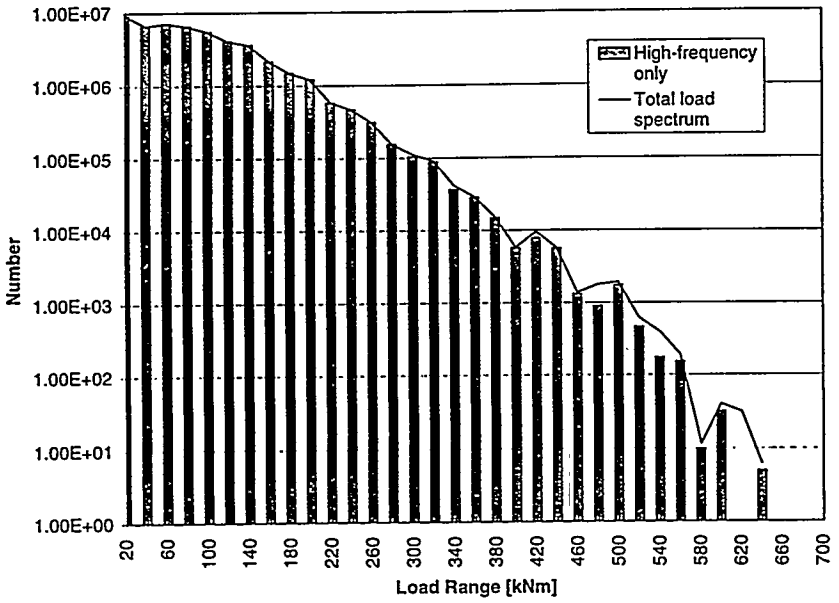

Figure 13. Traditional– and total one year load spectra for the rotor tilt moment (not accumulated).

In Fig. 14, the similar results are displayed in terms of accumulated load spectra.

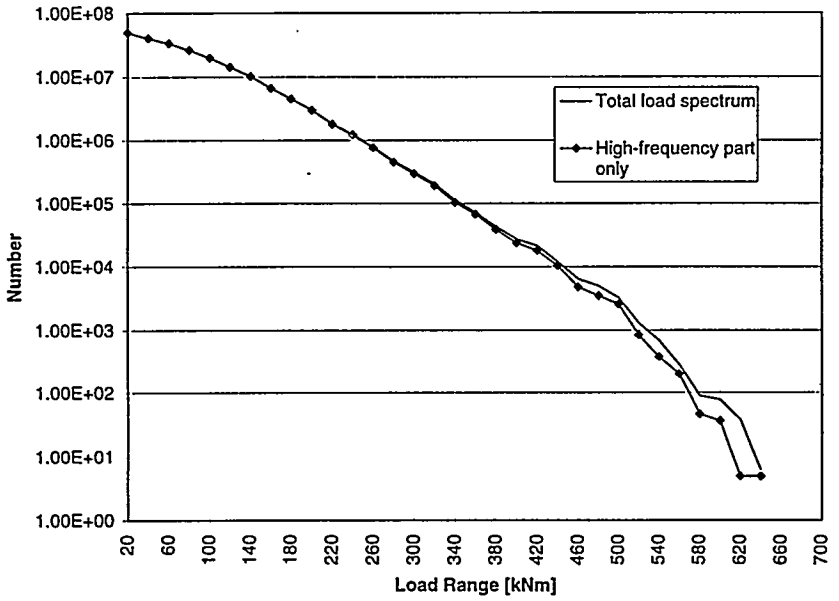

Figure 14. Traditional– and total accumulated one year load spectra for the rotor tilt moment.

It appears from the figure that the parts related to moderate range sizes are very similar for the traditional– and for the total load spectrum. However, the parts associated with large load ranges differ considerable[6].

[6]The added low frequency contribution originates mainly from transitions between the basic load cases due to the lack of 10–minutes mean wind speed values above the cut–out wind speed in the selected reference year, and due the the moderate load ranges introduced with the transients related to the cut–in mean wind speed.

The above difference expressed in terms of fatigue life consumption is shown in Table 4, where the equivalent load ranges (based on an equivalent number of load ranges equal to 10^6) are established by applying the Palmgren–Miner rule with the Wöhler exponents m = 3, m = 7, and m = 12.

m	Traditional load spectrum	Total load spectrum	Ratio
3	443.13 kNm	444.96 kNm	1.00
7	315.07 kNm	318.68 kNm	1.01
12	340.66 kNm	347.36 kNm	1.02

Table 4. Equivalent tilt load ranges based on traditional– and total load spectra for various Wöhler exponents.

The damage ratios, corresponding to the listed ratios of equivalent load ranges shown in Table 4, are determined to 1.01, 1.08, and 1.26, respectively.

The relative importance of the individual load ranges is illustrated on Fig. 15, Fig. 16, and Fig. 17 for different values of the Wöhler exponent. Each of the figures show the relative lifetime consumption of a particular load range.

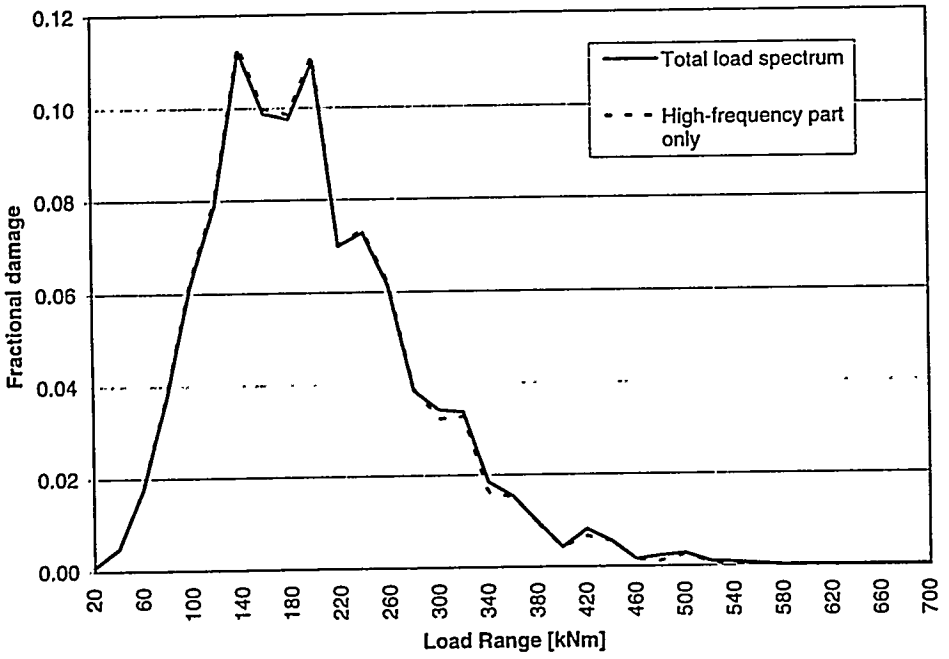

Figure 15. Relative fatigue lifetime consumption for the traditional– and the total load spectrum for m = 3.

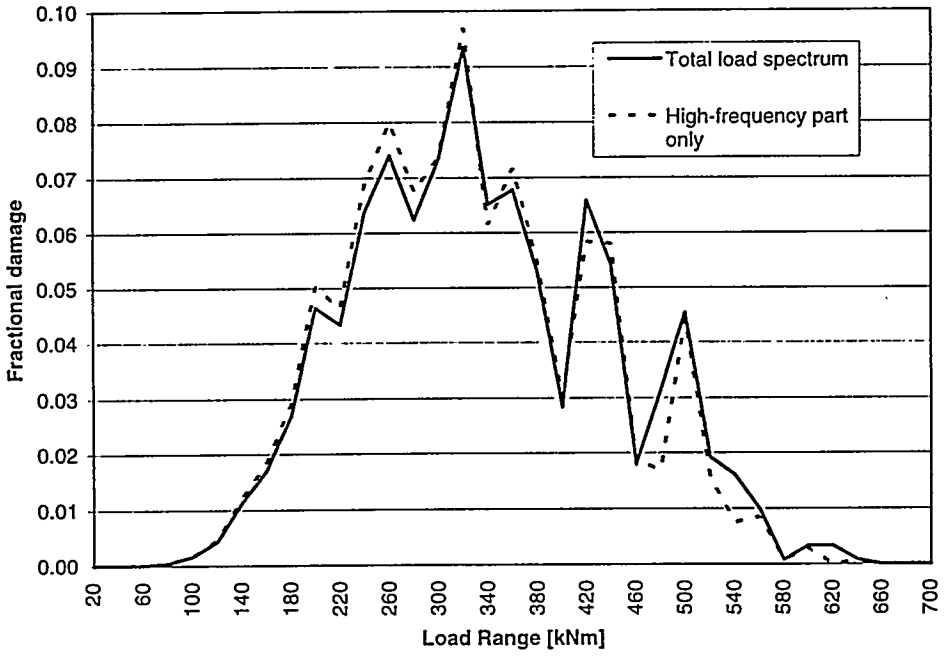

Figure 16. Relative fatigue lifetime consumption for the traditional- and the total load spectrum for m = 7.

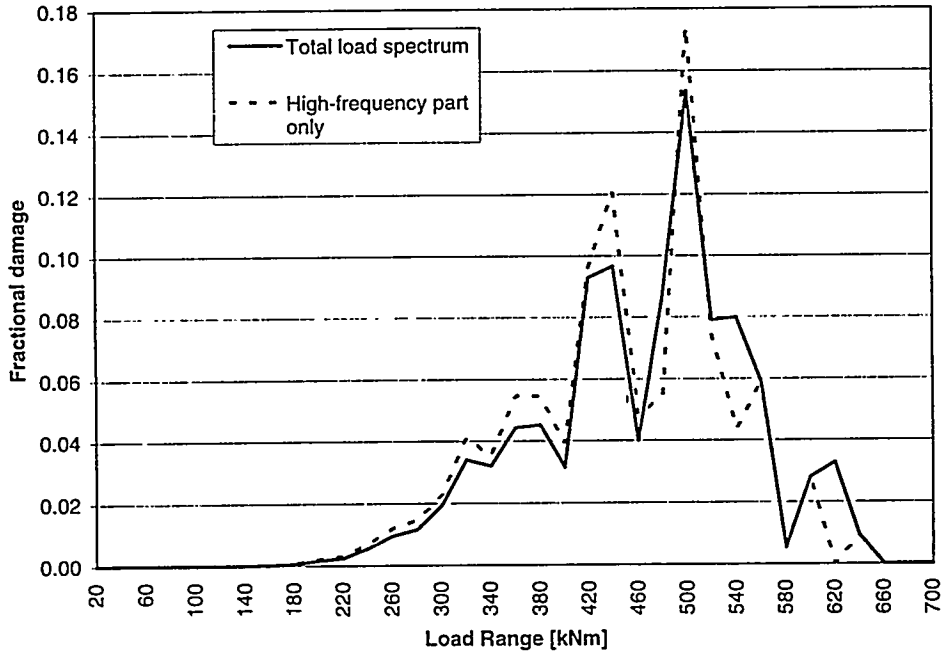

Figure 17. Relative fatigue lifetime consumption for the traditional- and the total load spectrum for m = 12.

As the main difference between the traditional– and the total load spectrum is attached to a relative limited number of relative large load ranges, it is expected that the most distinct difference between the curves describing the relative lifetime consumption relates to large Wöhler exponents. This is confirmed by the analyses.

6 Conclusion

A framework for an approximative inclusion of low–frequency contributions, originating from the transition between the basic load cases in the duty cycle description, has been established. The algorithm allows inclusion of both contributions associated with transient load cases and production load cases. In the present formulation, the procedure is based on an application of the rainflow counting method in combination with the Palmgren–Miner fatigue approach. For very low frequencies, application of the Palmgren–Miner rule might introduce some conservatism in the fatigue estimate.

The method has been applied to a demonstration example consisting of simulated load events associated with a rotor tilt– and a blade flapwise moment on a conventional wind turbine during a one year period. The low–frequency contribution is shown to add a limited number of relative large load ranges to the traditional load spectrum. As all the 10–minutes mean wind speed values, constituting the selected reference year, are below the cut–out wind speed (25 m/s) and as transient situations related to the cut–in wind speed introduce only moderate load ranges, the present low frequency contribution originates mainly from transitions between the basic load cases.

In terms of equivalent moments, the low–frequency part of the flapwise moment account for approximately 8%/1% for relative large/small Wöhler exponents, corresponding to a reduction in the lifetime by approximately 60%/3%. Conserning the rotor tilt moment, the low–frequency part contribution to the equivalent moment is approximately 2%/.4% for relative large/small Wöhler exponents, corresponding to a reduction in the lifetime by approximately 21%/1%.

References

[1] IEC 1400–1, Safety of Wind Turbine Generator Systems. International Electrotechnical Commission, 1994–05–27.

Bibliographic Data Sheet **Risø–R–913(EN)**

Title and author(s)

Low Cycle Fatigue Loads

Gunner C. Larsen and Kenneth Thomsen

ISBN
87–550–2204–9

ISSN
0106–2840

Dept. or group
Test Station for Wind Turbines
Dept. of Meteorology and Wind Energy

Date
August 1996

Groups own reg. number(s)
PFV–03908–01

Project/contract No.
ENS–1363/94–0002

Pages	Tables	Illustrations	References
21	4	17	1

Abstract (Max. 2000 char.)

A simple approximative algorithm for taking into account low cycle fatigue loads, related to transitions between the basic load cases forming the traditional duty cycle description, is outlined. The algorithm allows inclusion of contributions associated with both transient load cases and production load cases. In the present formulation, the procedure is based on an application of the rainflow counting method as well as the Palmgren–Miner fatigue approach.

The method has been applied to a demonstration example consisting of simulated load events associated with flap– and tilt moments on a conventional wind turbine during a one year period. For the most critical component, the low–frequency contribution is shown to add approximately 10% to the equivalent moment, corresponding to a reduction in lifetime by approximately 60%.

Descriptors INIS/EDB

COMPUTERIZED SIMULATION; DYNAMIC LOADS; FATIGUE; ROTORS; SERVICE LIFE; STRUCTURAL MODELS; WIND LOADS; WIND TURBINES

Available on request from:
Information Service Department, Risø National Laboratory (Afdelingen for Informationsservice, Forskningscenter Risø)
P.O. Box 49, DK–4000 Roskilde, Denmark
Phone (+45) 46 77 46 77, ext. 4004/4005 · Telex 43 116 · Fax (+45) 46 75 56 27